Separation Science and Technology
Publication details, including instructions for authors and subscription information:
http://www.informaworld.com/smpp/title~content=t713708471

Absorption of Carbon Dioxide into Ionic Liquid of 2-Hydroxy Ethylammonium Lactate

Bung-Jin Hwang[a]; Sang-Wook Park[a]; Dae-Won Park[a]; Kwang-Joong Oh[a]; Seong-Soo Kim[b]
[a] Division of Chemical Engineering, Pusan National University, Busan, Korea [b] School of Environmental Science, Catholic University of Pusan, Busan, Korea

To cite this Article Hwang, Bung-Jin , Park, Sang-Wook , Park, Dae-Won , Oh, Kwang-Joong and Kim, Seong-Soo(2009) 'Absorption of Carbon Dioxide into Ionic Liquid of 2-Hydroxy Ethylammonium Lactate', Separation Science and Technology, 44: 7, 1574 — 1589

To link to this Article: DOI: 10.1080/01496390902775778

URL: http://dx.doi.org/10.1080/01496390902775778

Separation Science and Technology, 44: 1574–1589, 2009

ISSN: 0149-6395 print/1520-5754 online
DOI: 10.1080/01496390902775778

Absorption of Carbon Dioxide into Ionic Liquid of 2-Hydroxy Ethylammonium Lactate

Bung-Jin Hwang,[1] Sang-Wook Park,[1] Dae-Won Park,[1]
Kwang-Joong Oh,[1] and Seong-Soo Kim[2]
[1]Division of Chemical Engineering, Pusan National University,
Busan, Korea
[2]School of Environmental Science, Catholic University of Pusan,
Busan, Korea

Abstract: Absorption of carbon dioxide into organic solvents such as DMA, NMP, DMSO, and DMF with the 2-hydroxy ethylammonium lactate (HEAL) ionic liquid was investigated using a batch stirred tank with a plane of gas-liquid interface in a range of 0–2.0 kmol/m^3 of HEAL and 298–318 K at 101.3 kPa. The absorption of CO_2 was analyzed with the film model accompanied by the zwitter-ion mechanism of CO_2 with HEAL. The proposed model fits the experimental data of the enhancement factor due to the ready, chemical absorption of CO_2 in different solvents, temperatures, and HEAL concentrations. The reaction rate constant of CO_2 with HEAL was correlated linearly with the solubility parameter of the solvent.

Keywords: Absorption, carbon dioxide, 2-hydroxy ethylammonium lactate, ionic liquid

INTRODUCTION

Carbon dioxide (CO_2) produced by combustion of fossil fuels is regarded as the most significant greenhouse gas with its increasingly accumulation

Received 7 July 2008; accepted 9 January 2009.

Address correspondence to Sang-Wook Park, Division of Chemical Engineering, Pusan National University, Busan 609-735, Korea. E-mail: swpark@pusan.ac.kr

in the atmosphere attracting worldwide attention. Conversely, CO_2 is one of the most naturally abundant, inexpensive, non-flammable, and non-toxic C1 resources (1). To utilize CO_2 as C1 feedstock or sequestrate it for reduction in the greenhouse effect, investigation into efficient methods for capturing it from flue gas is critically important. One of the most commercially applied technologies is the chemical absorption of CO_2 by aqueous amines (2). Although many studies have been done on the mechanisms and kinetics of the reaction between CO_2 and various amines, the reaction media are currently limited to aqueous solutions. In practice, non-aqueous systems comprising methanolic solutions of alkanolamine have been commercially employed for CO_2 absorption because of their high solubility and capacity, low corrosiveness, and low energy consumption during generation of used liquor (2). With either mode of gas removal, the vapor pressure of the solvent itself plays a significant role in the gas-liquid processes, usually to their detriment with solvent into the gas stream being particularly problematic. Compounding this issue is the loss of the volatile, amine sequestering agent into the gas stream.

A liquid that could facilitate the sequestration of gases without concurrent loss of the captured agent or solvent into the gas stream would prove to be a superior material in such applications. In this regard, ionic liquids show great potential as an alternative for such application due to the Coulombic attraction between the ions of liquid that exhibit no measurable vapor pressure up to their thermal decomposition point, generally >300°C. This lack of vapor pressure makes these materials highly attractive for gas processing (3). In recent years, significant progress has been made in the application of ionic liquids as alternative solvents and catalysts due to their unique properties of vapor pressure, a broad range of liquid temperatures, excellent thermal and chemical stabilities, and tunable physicochemical characteristics (4). Bates et al. (5) presented the possibility of an imidazolium bromide ionic liquid as a reactant to capture CO_2, the reaction mechanism, and measured the molar uptake of CO_2 per mole of the ionic liquid as approaching 0.5, the theoretical maximum for CO_2 sequestration as an ammonium carbamate salt during the 3 hours exposure period. Thus, the aim of this work is to examine the effect of the 2-hydroxy ethylammonium lactate ionic liquid on the absorption rates of CO_2 in non-aqueous solutions such as *N,N*-dimethylacetamide, *N*-methyl-2-pirrolidinone, dimethyl sulfoxide, and *N,N*-dimethylformamide, using the film theory accompanied by the zwitterion mechanisms of the reaction between CO_2 and 2-hydroxy ethylammonium lactate.

THEORY

The overall reaction between CO_2 (A) and 2-hydroxy ethylammonium lactate (HEAL, B) using the reaction scheme, proposed by Bates et al. (5) as a template, is as follows:

$$\begin{aligned} &CO_2 + 2R_1(R_1)(R_2)NH^+X^- \\ &\quad\longrightarrow R_1(R_2)NCOO^- + R_1(R_1)(R_2)NH^+ + 2HX \end{aligned} \qquad \text{(i)}$$

where R_1, R_2, and X- are –H, $-CH_2CH_2OH$, and $-OOCCH_2(OH)CH_3$, respectively.

In 1979 Danckwerts (6) reintroduced a mechanism originally proposed in 1968 by Caplow (7) to explain the reported differences in the orders of the reaction of CO_2 with primary amine. This reaction mechanism involved two steps: the formation of a reactive zwitterion intermediate and the subsequent removal of a proton by a base.

Assuming that the overall reaction (i) consists of two steps, the following reaction mechanism is proposed:

$$CO_2 + R_1(R_1)(R_2)NH^+X^- \underset{k_2}{\overset{k_1}{\longleftrightarrow}} R_1(R_1)(R_2)N^+COO^- + HX \qquad \text{(ii)}$$

$$\begin{aligned} &R_1(R_1)(R_2)N^+COO^- + R_1(R_1)(R_2)NH^+ + X^- \\ &\xrightarrow{k_3} (R_1)(R_2)NCOO^- + R_1(R_1)(R_2)NH^+HX \end{aligned} \qquad \text{(iii)}$$

In the above reactions, the first step takes place instantaneously with the second step being bimolecular, second-order, and rate-determining.

In the case of non-aqueous solvents, only the amine is considered as the base in the proton removal step (8). If the steady state approximation is applied to the zwitterion, one gets a rate of homogeneous reaction as:

$$r_A = \frac{C_A C_B}{1/k_1 + k_2/(k_1 k_3 C_B)} \qquad (1)$$

The material balances for species A and B based on the film theory accompanied by the reaction rate of Eq. (1) and the boundary conditions can be written as

$$D_A \frac{d^2 C_A}{dz^2} = \frac{C_A C_B}{1/k_1 + k_2/(k_1 k_3 C_B)} \qquad (2)$$

$$D_B \frac{d^2C_B}{dz^2} = \frac{C_A C_B}{1/k_1 + k_2/(k_1 k_3 C_B)} \tag{3}$$

$$z = 0, \quad C_A = C_{Ai}, \quad \frac{dC_B}{dz} = 0$$

$$z = z_L, \quad C_A = 0, \quad C_B = C_{Bo}$$

Enhancement factor (β) here is defined as the ratio of molar flux ($-D_A dC_A/dz$) with a chemical reaction to that ($D_A C_{Ai}/z_L$) without chemical reaction at gas-liquid interface:

$$\beta = -\left.\frac{da}{dx}\right|_{x=0} \tag{4}$$

where a and x are C_A/C_{Ai} and z/z_L, respectively.

If the absorption process is conducted under conditions where the liquid phase reaction may be considered first-order with respect to CO_2, using the pseudo-first-order model, the rate of reaction for CO_2 will be given as follows:

$$r_A = k_o C_A \tag{5}$$

where the pseudo-first-order reaction rate constant (k_o) is defined, according to Eq. (1), as:

$$k_o = \frac{C_{Bo}}{1/k_1 + k_2/(k_1 k_3 C_{Bo})} \tag{6}$$

The material balance of species A and the boundary conditions by the film model based on Eq. (5) can be written as:

$$D_A \frac{d^2C_A}{dZ^2} = k_o C_A \tag{7}$$

$$z = 0, \quad C_A = C_{Ai}; \qquad z = z_L, \quad C_A = 0 \tag{8}$$

The enhancement factor (β) from the exact solution of Eq. (7) and Eq. (4) was derived as:

$$\beta = \frac{\sqrt{k_o D_A}/k_{Lo}}{\tanh(\sqrt{k_o D_A}/k_{Lo})} \tag{9}$$

The value of k_o was obtained from the experimental data of $\beta(\beta_{exp})$ using Eq. (9).

Eq. (6) was rearranged as follows:

$$\frac{C_{Bo}}{k_o} = \frac{1}{k_1} + \frac{k_2}{k_1 k_3 C_{Bo}} \tag{10}$$

Thus, k_1 and k_2/k_3 were obtained from the intercept and slope of the plots of C_{Bo}/k_o vs. $1/C_{Bo}$.

EXPERIMENTAL

Chemicals

All chemicals such as monoethanolamine, lactic acid, *N,N*-dimethylacetamide (DMA), *N*-methyl-2-pirrolidinone (NMP), dimethyl sulfoxide (DMSO), and *N,N*-dimethylformamide (DMF) were reagent grade, and used without further purification. Purity of CO_2 was more than 99.9%.

Synthesis of HEAL

HEAL was prepared by neutralization of monoethanolamine in ethanol with lactic acid along the same procedure as that reported by Yuan et al. (9) as follows:

0.5 mol of 2-amino ethanol was dissolved in 100 ml of ethanol to form a liquid mixture and loaded into a 500 ml flask. The flask was placed in a water bath of 298 K and equipped with a reflux condenser under vigorous stirring with a magnetic stirrer. A mixture of 0.5 mol of lactic acid dissolved in 100 ml of ethanol was added dropwise to the flask in about 90 min. The reaction lasted for 2 hours. The solvent was removed by evaporation under vacuum. The resulting crude residue was dissolved in 100 ml of ethanol, treated with activated carbon and filtered. A colorless product (HEAL) was obtained after evaporation and dried under vacuum at 323 K for 48 hours. The water mass fraction in HEAL after drying was less than 1×10^{-4} measured by Karl Fisher.

HEAL was characterized by FT-IR spectra were taken by a Perkin-Elmer IR spectrometer, using a NaCl disk. The presence of HEAL was confirmed to be the same by instrumental analysis, such as FT-IR (cyclic carbonate $C=O$ peak at $1800\,cm^{-1}$) and ^{13}C-NMR(cyclic carbonate $C=O$ at 160 ppm) spectra, which were as same as those measured in previous studies (9).

Absorption Rate of CO_2

The absorption rate of CO_2 was obtained by measurement of the pressure reduction of CO_2 according to the change of absorption time in a closed stirred cell absorber. Experimental setup used in this study was similar to that described by Alper et al. (10), shown in Fig. 1. The experiments were carried out in an absorber (0.7958 dm^3), consisting of a gas supply vessel (0.5884 dm^3) and a stirred-cell reactor (0.4074 dm^3 and inside diameter $= 0.063$ m). The pressure in the gas phase of the reactor was measured with a digital absolute pressure gauge (Merigauge: Scott Fetzer Company) with 1 place of decimal of a unit of mmHg. Four equally spaced vertical baffles, each one-tenth the reactor diameter in width, were attached to the internal wall of the reactor. Because pure CO_2 gas was used, only the liquid phase was stirred at 50 rpm by a magnetic stirrer. At this stirring speed, the surface of the liquid appeared to be without ripples. The gas-liquid interfacial area (3.077×10^{-3} m^2) was obtained as a ratio of the given liquid volume (0.2 dm^3) to the measured height of the liquid (0.065 m). Both the saturator and the absorber were kept in the water bath.

A known amount of freshly degassed liquid (200 dm^3) was poured into the reactor, after which the liquid was degassed again by applying vacuum for a few minutes to remove air potentially present before beginning the absorption of CO_2. Next, the liquid was allowed to equilibrate to a desired temperature, at which point the pressure controller was set to the desired (total) pressure and subsequently CO_2 allowed to flow from

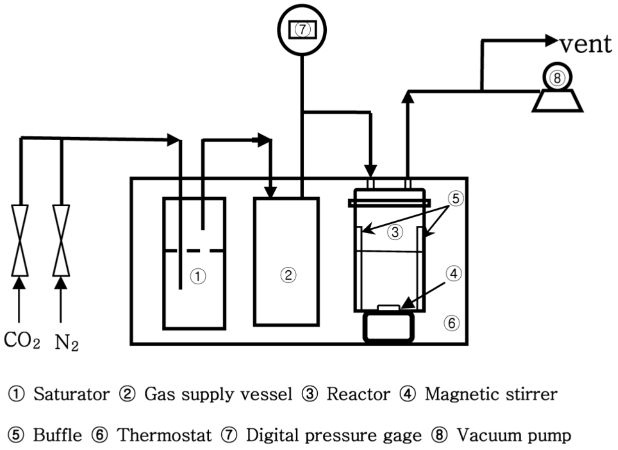

Figure 1. Schematic of the stirred cell absorber.

the gas supply vessel to the reactor. Next, the stirred-in liquid phase was switched on and the pressure decrease in the gas supply vessel, due to the CO_2 absorption, was read as a function of time. The actual pressure (P_A) of CO_2 in the gas phase was obtained from the measured total pressure (P) by subtracting the vapor pressure of the solvent. P was measured according to the change of time for various solvents (DMA, NMP, DMSO, and DMF), HEAL concentrations (0.5–2.0 kmol/m^3), and temperatures (298 −318 K), at 101.3 kPa to obtain β_{exp}.

Physical Properties

The solubility of CO_2 (C_{Ai}), diffusivity (D_{iS} and D_i) of CO_2, and mass transfer coefficient (k_{Lo}) of CO_2 in the solvent, required to solve the differential equations of Eq. (2) and (3), were obtained as follows:

C_{Ai} was measured by the pressure measuring method, which involved measuring the pressure difference of CO_2 before and after equilibrium in the gas and liquid phases, similar to the procedure previously reported (11), and the experimental procedure was duplicated in detail as previously ported (12).

The liquid viscosity (μ) was measured using Brookfield viscometer (Brookfield Eng. Lab. Inc, USA).

D_i of species i in liquid phase was estimated by the method modified with viscosity in Stoke-Einstein equation (13) as follows:

$$D_i = 7.4 \times 10^{-12} \frac{TM_S^{1/2}}{\mu^{2/3} V_i} \tag{11}$$

The experimental data (14) were better correlated through the use of two-thirds power of viscosity in Eq. (11) rather than one power as shown in Stoke-Einstein equation.

From measurement of the pressure change of CO_2 according to the change of time in the closed vessel (Fig. 1), the instantaneous mass balance (10) with a constant gas volume (V_G) and at constant temperature gives:

$$N_A = -\frac{V_G}{RTS_o} \frac{dP_A}{dt} \tag{12}$$

It should be noted that N_A is presented as follows:

$$N_A = k_L(C_{Ai} - C_A) \tag{13}$$

Using Eqs. (12) and (13), and Henry's law, k_L at the initial time is obtained:

$$k_L = \frac{V_G H_A}{RTS_o}\left(-\frac{d \ln P_A}{dt}\right)_{t=0} \tag{14}$$

where H_A is the Henry's constant at the initial partial pressure of CO_2.

The values of the mass transfer coefficient (k_{Lo}) of CO_2 in various solvent were obtained from Eq. (14).

The values of μ, C_{Ai}, D_{AS}, D_{BS}, and k_{Lo} are listed in Table 1.

RESULTS AND DISCUSSION

Measurement of Enhancement Factor (β_{exp})

Generally, β_{exp} due to the chemical reaction in gas absorption was obtained as the ratio of the absorption rate with reaction to that without reaction, or the ratio of the liquid-side mass transfer coefficient (k_{LR}) of gas with reaction to that (k_{Lo}) without reaction (15). β_{exp} in this study was obtained from the ratio of k_{LR} to k_{Lo} using Eq. (14).

The typical plots of P_A against absorption time were shown in Fig. 2 in a semi-logarithmic form for solvent DMSO with C_{Bo} of 0 and 2.0 kmol/m^3 at 298 K.

The plots in Fig. 2 were analyzed using the multiple nonlinear regression method to give the slope of at an initial time, thus, k_{Lo} and k_{LR}

Table 1. Physical properties of the CO_2/HEAL system

T(K)	Solvent	C_{Ai} (kmol/m^3)	μ (cp)	D_{AS}x10^9 (m^2/s)	$D_{BS} \times 10^9$ (m^2/s)	$k_{Lo} \times 10^5$ (m/s)
298	DMA	0.064	1.0330	2.426	0.934	3.295
	NMP	0.062	1.7600	1.814	0.699	1.817
	DMSO	0.055	2.1190	1.423	0.548	1.812
	DMF	0.066	0.8996	2.437	0.939	3.315
308	DMA	0.059	0.9274	2.694	1.038	3.539
	NMP	0.061	1.5441	2.046	0.788	1.970
	DMSO	0.054	1.8289	1.622	0.625	1.977
	DMF	0.062	0.8369	2.643	1.018	3.499
318	DMA	0.059	0.8527	2.942	1.133	3.728
	NMP	0.061	1.3825	2.274	0.876	2.113
	DMSO	0.053	1.5414	1.877	0.723	2.180
	DMF	0.062	0.7663	2.894	1.114	3.717

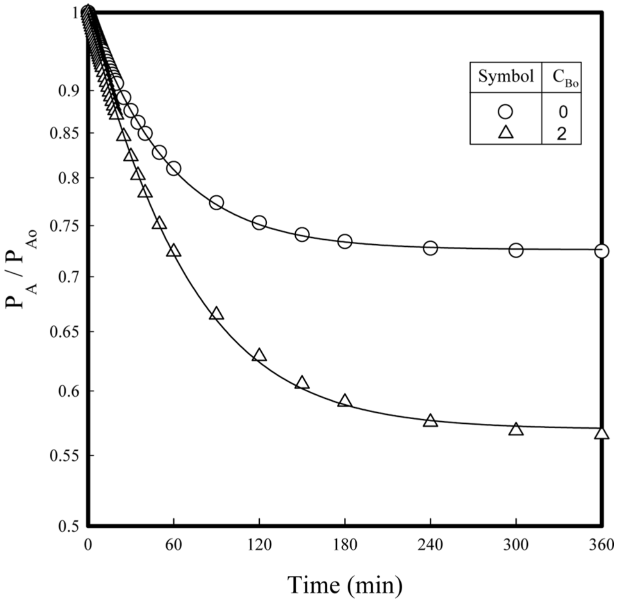

Figure 2. P_A/P_{Ao} vs. time in DMSO solvent of $C_{BO} = 0$ and 2.0 kmol/m^3 at 298 K.

obtained by Eq. (14) were 1.812×10^{-5} m/s and 2.524×10^{-5} m/s, respectively.

The physical mass transfer coefficient (k_L) in reactant HEAL solution can not be measured because of a reaction of CO_2 with HEAL. In this study, the relationship between the mass transfer coefficient (k_{Lo}) in solvent and diffusivity ratio of D_A to D_{AS} was used to obtain as following (16):

$$k_L = k_{Lo}(D_A/D_{AS})^{2/3} \tag{15}$$

In the case of Fig. 2, k_L for C_{Bo} of 2.0 kmol/m^3 was 1.139×10^{-5} m/s using k_{Lo} in Table 1,from which β_{exp} was 2.216.

Figure 3 shows the plots of β_{exp} against C_{Bo} at a typical temperature of 298 K with symbols for various solvents.

As shown in Fig. 3, β_{exp} increases with increasing C_{Bo} and temperature. These results are exhibited equally for other solvents. The solid line presents the calculated value (β_{cal}) of β, to be discussed later.

To obtain the reaction rate constants, k_o were obtained using β_{exp} and Eq. (9) in the range of 0.5–2.0 kmol/m^3 of HEAL for various

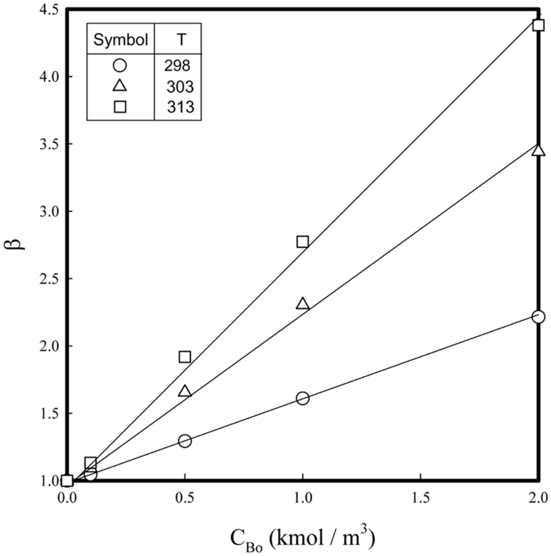

Figure 3. Enhancement factor vs. C_{Bo} in DMSO solvent at various temperatures.

solvents and temperatures. Plots of C_{Bo}/k_o against $1/C_{Bo}$ are presented for various solvents at a typical temperature of 298 K in Fig. 4.

As shown in Fig. 4, the plots satisfy a straight line, with the values of k_1 and k_2/k_3, according to Eq. (10), obtained from the intercept and slope of the straight line, respectively. These results are exhibited equally at 308 and 318 K. The values of k_1 and k_2/k_3 for various solvents and temperatures are listed in Table 2.

Figure 5 shows the Arrhenius plots of the values of k_1 using data in Table 2.

As shown in Fig. 5, the Arrhenius plots are linear and the linear regression analysis of the Arrhenius plots with $r^2 > 0.960$ gives the activation energy for forward reaction rate constant in the reversible reaction of (ii); i. e., 15.1, 22.8, 66.0, and 74.2 kJ/mol for DMA, NMP, DMSO, and DMF, respectively.

Various empirical measurements of the solvent effect have been proposed and correlated with the reaction rate constant (17). Of these, some measurements have a linear relation to the solubility parameter (δ) of the solvent with logarithms of k_1, k_2/k_3 plotted against δ (18) of DMA, NMP, DMSO, and DMF of 22.1, 23.1, 24.6, and 24.6 $(J/m^3)^{0.5}$, respectively, in Fig. 6.

As shown in Fig. 6, the plots are linear, and k_1 and k_2/k_3 increase and decrease with increasing δ, respectively. The solvent polarity is

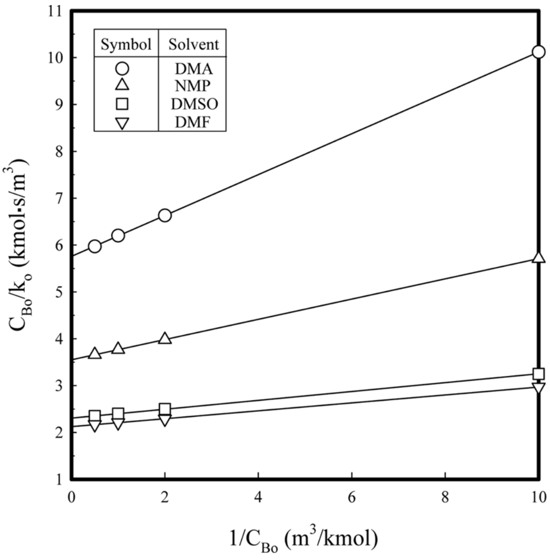

Figure 4. C_{Bo}/k_o vs. $1/C_{Bo}$ for various solvents at 298 K.

increased with increasing δ. It can be assumed that increased unstability and solvation of $R_1(R_1)(R_2)N^+COO^-$ (C_1), arising from the increased solvent polarity, enhance the dissociation reaction of C_1 and the reaction between C_1 and CO_2, such as SN_1(nucleophilic substitution) (19), respectively. The values of k_1 and k_2/k_3 decreased upon increasing δ, as shown

Table 2. Reaction rate constants of reaction between CO_2 and HEAL

T(K)	Solvent	k_1 (m^3/kmol · s)	k_2/k_3 (m^3/kmol)
298	DMA	0.1738	0.0758
	NMP	0.2816	0.0608
	DMSO	0.4337	0.0410
	DMF	0.4703	0.0397
308	DMA	0.3675	0.1052
	NMP	0.5513	0.0939
	DMSO	1.1806	0.0724
	DMF	1.2965	0.0664
318	DMA	0.5574	0.1441
	NMP	0.8601	0.1245
	DMSO	2.1101	0.1056
	DMF	2.3564	0.1025

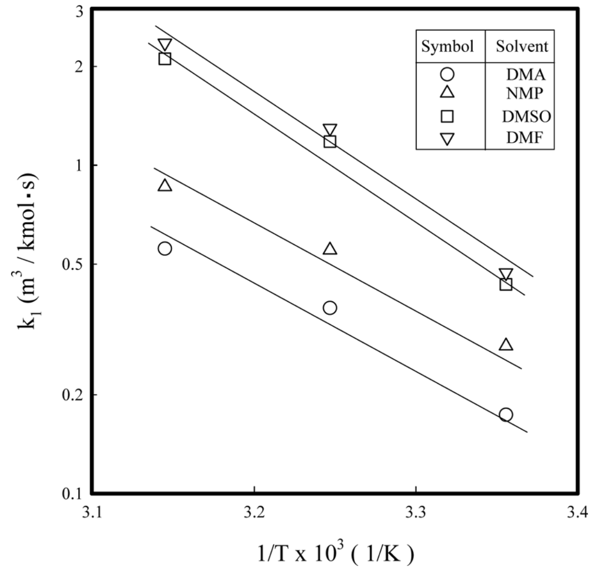

Figure 5. Arrhenius plot of the CO_2-HEAL system.

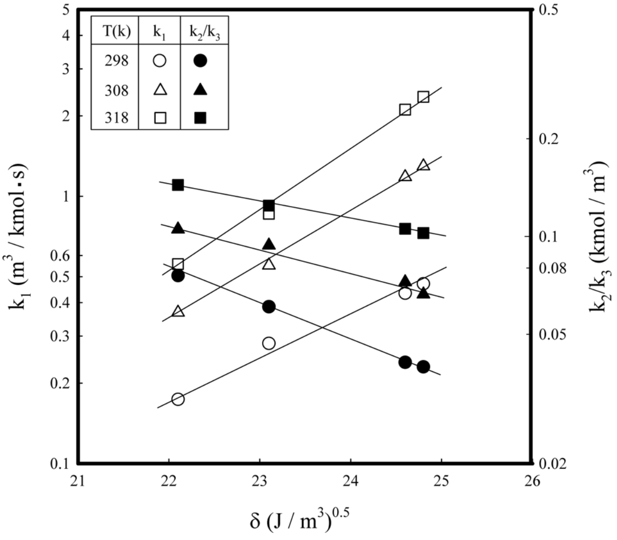

Figure 6. Relationship between reaction rate constant and various solvent solubilities at 298 K.

in Fig. 6, thus, the magnitude of the rate constants may be a function of the degree to which the solvent was able to stabilize the zwitterions intermediate (15).

Using the obtained values of k_1 and k_2/k_3 at the given C_{Bo}, C_{Ai}, D_A, D_B, and k_{Lo} in Table 1, Eq. (2) and (3) were numerically solved using a finite element method of FEMLAB$^@$ to give the profiles of C_A and C_B. The typical profiles of C_B for various C_{Bo} in the DMA and DMSO solution at 298 K were shown in Fig. 7.

As shown in Fig. 7, the values of C_B/C_{Bo} at the gas-liquid interface were larger than 0.9, from which the reaction between CO_2 and HEAL could be assumed to be a pseudo-first-order reaction with respect to the concentration of CO_2.

The theoretical value (β_{cal}) of β was calculated from Eq. (4) and the concentration profile of CO_2, obtained from a numerical solution of Eq. (2) and (3) for various solvents and HEAL concentrations, and is shown as symbols of solid line in Fig. 3. As shown in Fig. 3, β_{exp} approached to β_{cal}.

All values of β_{exp} and β_{cal} for HEAL concentrations (0.5–2.0 kmol/m^3) and temperatures (298–318 K) in various solvents were plotted in Fig. 8 to compare each other. As shown in Fig. 8, β_{exp} approach to β_{cal} within a mean deviation of 4.45% with r^2 of 0.952.

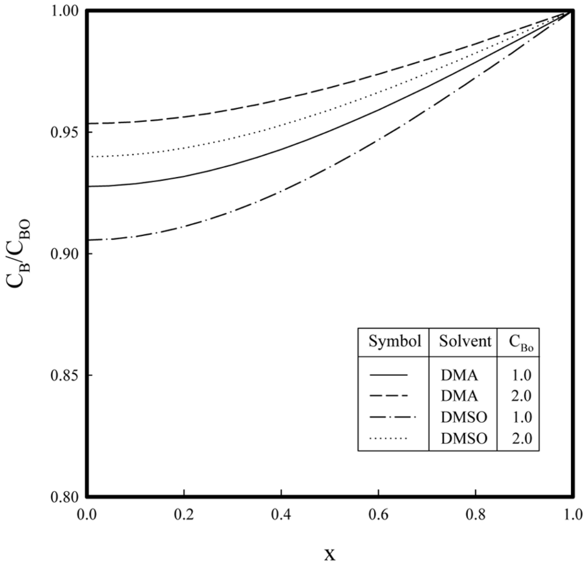

Figure 7. Dimensionless concentration profiles of HEAL in the liquid film.

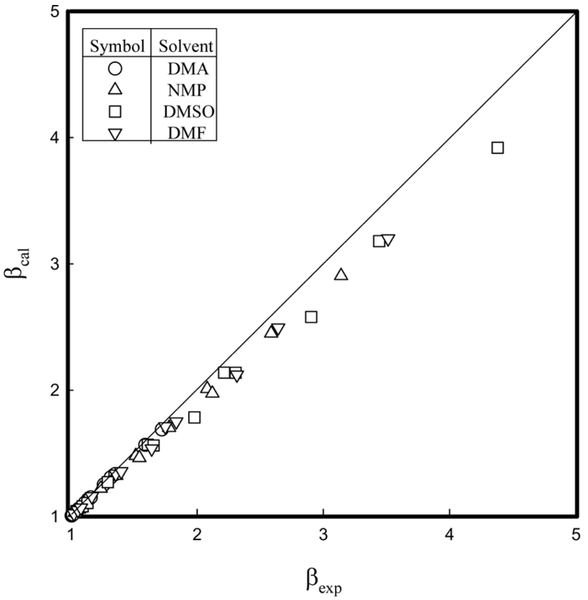

Figure 8. Comparison of the calculated and measured values of enhancement factor of CO_2.

CONCLUSIONS

Carbon dioxide was absorbed into a HEAL solution of solvents such as DMA, NMP, DMSO, and DMF in a flat stirred vessel at 101.3 kPa. A mathematical model for the CO_2 absorption accompanied by its reaction with HEAL was developed on the basis of the film theory with a nonlinear reaction rate equation according to the zwitterions mechanism. Absorption data of CO_2 were used to obtain pseudo-first-order reaction rate constant, from which the elementary reaction rate constants were evaluated. It was found that the dependence of the logarithms of the reaction constants on the solubility parameter of the solvent was close to linear.

ACKNOWLEDGEMENTS

This work was supported by Brain Korea 21 Project and a grant (2006-C-CD-11-P-03–0-000–2007) from the Energy Technology R&D of Korea Energy Management Corporation. Dae-Won Park is also thankful for KOSEF (R01–2007-000–10183-0).

NOMENCLATURE

C_i : concentration of species i (kmol/m^3)
D_i : diffusivity of species i (m^2/s)
H_A : Henry constant of CO_2 in solvent (atm·m^3/kmol)
k_o : pseudo-first-order reaction rate constant (1/s)
k_1 : forward reaction rate constant in reaction (ii) (m^3/kmol·s)
k_2 : backward reaction rate constant in reaction (ii) (1/s)
k_3 : forward reaction rate constant in reaction (iii) (m^3/kmol·s)
k_L : liquid-side mass transfer coefficient of CO_2 (m/s)
k_{Lo} : liquid-side mass transfer coefficient of CO_2 without reaction (m/s)
k_{LR} : liquid-side mass transfer coefficient of CO_2 with reaction (m/s)
P_A : pressure of CO_2 in the gas phase (atm)
r^2 : correlation coefficient
r_A : reaction rate of CO_2 (kmol/m^3·s)
S_o : interfacial area of liquid (m^2)
t : absorption time (s)
T : absorption temperature (K)
V_G : volume of gas in the absorber (m^3)
z : distance (m)
z_L : film thickness(m)

Greek Letters

β : enhancement factor of CO_2
δ : solubility parameter of solvent $(J/m^3)^{1/2}$
μ : viscosity of liquid (cP)

Subscripts

A : CO_2
B : HEAL
G : gas phase
L : liquid phase
S : solvent
I : gas-liquid interface or species i
o : feed or initial time

REFERENCES

1. Aresta, M. (2003) *Carbon Dioxide Recovery and Utilization*; Kluwer Academic Pub.: Boston.
2. Astarita, G.; Savage, D. W.; Bisio, A.. (1983) *Gas Treating with Chemical Solvents*; John Wiley & Sons: New York.

3. Zhang, S.; Sun, N.; He, X.; Lu, X.; Zhang, X. (2006) Physical properties of ionic liquids: Database and evaluation. *J. Phys. Chem. Ref. Data*, *35*: 1475.
4. Rogers, R. D.; Seddon, K. R. (2005) *Ionic Liquids IIIA: Fundamentals, Progress, Challenges, and Opportunities*; ACS: Washington, DC.
5. Bates, E. D.; Mayton, R. D.; Ntai, I.; Davis, Jr., J. H. (2002) CO_2 capture by a task-secific ionoc liquid. *J. Am. Chem. Soc.*, *124*: 926.
6. Danckwerts, P. V. (1979) The reaction of CO_2 with ethanolamines. *Chem. Eng. Sci.*, *34*: 443.
7. Caplow, M. (1968) Kinetics of carbamate formation and breakdown. *J. Am.Chem. Soc. 90*: 6795.
8. Sada, E.; Kumazawa, H.; Han, Z. Q.; Matsuyama, H. (1985) Chemical kinetics on the reaction of carbon dioxide with ethanolamine in nonaqueous solvents. *AIChE J. 31*: 1297.
9. Yuan, X. L.; Zhang, S. J.; Lu, X. M. (2007) Hydroxy ammonium ionic liquids: Synthesis, properties, and solubility of SO_2. *J. Chem. Eng. Data*, *52*: 596.
10. Alper, E.; Al-Hamed, A.; Shaikh, A. A. (1987) Kinetics and selectivity of carbon dioxide absorption by aqueous methyl-diethanolamine solutions. *Proc. Int. Chem. React. Eng. Conf.*, *2*: 17.
11. Kennard, A.; Meisen, M. L. (1984) Solubility of carbon dioxide in aqueous diethanolamine solutions at elevated temperature and pressures. *J. Chem. Eng. Data*, *29*: 309.
12. Park, S. W. Park; Choi, B. S.; Lee, B. D.; Park, D. W.; Kim, S. S. Kim. (2006) Chemical absorption of carbon dioxide into glycidyl methacrylate solution with tetrabutylammonium bromide. *Sep. Sci., Technol.*, *41*: 829.
13. Reid, R. C.; Prausnitz, J. M.; Sherwwod, T. K. (1977) *The Properties of Gases and Liquid*; McGraw-Hill Book Company: New York.
14. Cussler, E. L. (1984) *Diffusion*; Cambridge University Press: New York.
15. Park, S. W.; Kim, K. W.; Sohn, I. J.; Kaseger, C. F. (2000) Facilitated transport of sodium phenolate through supported liquid membrane. *Sep. Purifi, Technol.*, *19*: 3.
16. Carta, G.; Pigford, R. L. (1983) Absorption of nitric oxide in nitric acid and water. *Ind. Eng. Chem. Fundam.*, *22*: 329.
17. Herbrandson, H. F.; Neufeld, F. R. (1966) Organic reactions and the critical energy density of the solvent. The solubility parameter as a new solvent parameter. *J. Org. Chem.*, *31*: 1140.
18. Brandrup, J.; Immergut, E. H. (1975) *Polymer Handbook*; Second Ed., John Wiley & Sons: New York.
19. Morrison, R. T.; Boyd, R. N. (1983) *Organic Chemistry;* Fourth Ed., Allyn and Bacon, Inc.: Toronto.
20. Park, S. W.; Choi, B. S.; Park, D. W.; Oh, K. J.; Lee. J. W. (2007) Chemical kinetics of carbon dioxide with glycidyl methacrylate using immobilized tributylamine supported on poly(styrene-co-vinylbenzyl chloride) as a catalyst. *Green Chem.*, *9*: 605.